—Original Article—

Collagen complexes increase the efficiency of iPS cells generated using fibroblasts from adult mice

Byung-Soo CHANG[1)]*, Yun-Jung CHOI[2)]* and Jin-Hoi KIM[2)]

[1)]*Department of Cosmetology, Hanseo University, Chungnam 356-706, Republic of Korea*
[2)]*Department of Animal Biotechnology, College of Animal Bioscience & Technology, Konkuk University, Seoul 143-701, Republic of Korea*

Abstract. Different interventions are being tested for restoration of the youthfulness of adult mouse-derived fibroblasts. However, fundamental issues, such as the decline of adult mouse-derived fibroblast activity with age, remain unresolved. Therefore, in this study, we examined whether treatment with collagen complexes has beneficial effects on the rejuvenation or reprogramming of adult mouse-derived fibroblasts. Further, we investigated the mechanisms of rejuvenation of adult mouse-derived fibroblasts during treatment with total collagen complexes. We isolated total collagen complexes from the tails of young mice and cultured adult mouse-derived fibroblasts with or without the collagen complexes. When compared with fibroblasts cultured without collagen complexes, adult-derived fibroblasts cultured with collagen complexes over five consecutive passages showed a more youthful state, expanded at a higher rate, and exhibited reduced spontaneous cell death. The fibroblasts cultured in the presence of collagen complexes also showed extensive demethylation in the promoter regions of cell cycle-related genes such as PCNA, increased proliferation, and decreased senescence. In addition, the efficiency of reprogramming of fibroblasts to become induced pluripotent stem (iPS) cells was significantly higher in young- and adult-derived fibroblasts cultured with collagen complexes than in adult-derived fibroblasts cultured alone. Furthermore, mechanistic evidence shows that genes involved in anti-proliferative pathways, including *Ink4a/Arf* locus genes and *p53*, were downregulated in fibroblasts exposed to collagen complexes. Interestingly, our results suggest that the rejuvenation process was mediated via the α2β1 integrin-dependent Bmi-1 pathway. Thus, collagen complexes both stimulate proliferation and inhibit cell death and growth arrest in fibroblasts, which appears to be a promising approach for improving the efficiency of reprogramming.
Key words: Aging, Collagen complexes, Induced pluripotent stem (iPS) cells, Mouse, Reguvenation, Reprogramming

Mouse and human somatic cells can be reprogrammed to become induced pluripotent stem (iPS) cells by viral transduction of four transcription factors, namely, Oct4 (POU domain class 5 transcription factor 1; Octamer-4), Sox2 (sex determining region Y-box 2), C-myc (avian myelocytomatosis viral oncogene homolog) and Klf4 (Krüppel-like factor 4) [1–6]. The clinical utility of this finding was severely compromised initially by two issues: a tendency of the cells to undergo malignant transformation [7], and the fact that only a small fraction of treated cells expressed all four factors [8]. Random integration of retroviral copies led to genetic heterogeneity, with only 0.001% to 0.01% of infected cells reprogramming to a pluripotent state. Subsequently, reprogrammed cells were selected on the basis of reactivation of endogenous pluripotency genes [7, 9] or by using morphological criteria [2, 8].

More recently, secondary reprogramming systems have minimized genetic variation among reprogrammed cells. Mouse [10] and human [11] somatic cells carrying a doxycycline (Dox)-inducible lentivirus that expresses Oct4, Sox2, Klf4 and C-myc have been successfully reprogrammed, generating secondary iPS cells with higher efficiency. This raised the possibility of using iPS cells for patient-specific regenerative medicine, given that they avoid the problems of immunological rejection and the ethical issues associated with embryonic stem cells (ESCs). However, a recent study demonstrated that expression of the four reprogramming factors triggers senescence by upregulating *Ink4a/Arf* locus gene expression, *p53* and CDK inhibitors *p16^{Ink4a}* and *p21^{CIP1}* [12]. Therefore, the low efficiency of iPS cell derivation has continued to be a major challenge.

One source of multiple homeostatic signals *in vivo* is the extracellular matrix (ECM), which provides a scaffold for tissues and regulates many fundamental cellular processes, such as proliferation, survival, migration, and differentiation [13–15]. Another research group reported that solubilizing type I collagen enhanced the differentiation of rat bone marrow stem cells [16]. The inhibition of endogenous collagen results in a gradual loss of ESC characteristics [17]. Further, Suh and Han [18] reported that collagen I stimulates self-renewal of mouse ESCs.

Cellular senescence involves genomic instability, telomere loss, oxidative damage, genetic programming, and cell death [12]. Recently,

researchers have become interested in designing effective methods for generating and reprogramming iPS cells. Therefore, in this study, we first examined whether treatment with collagen complexes has beneficial effects on the rejuvenation of skin fibroblasts obtained from adult mice. Second, cellular senescence was evaluated using senescence-associated beta-galactosidase (SA-βgal) and cell proliferation assays. Third, we explored the role of collagen complexes for enhancement of reprogramming efficiency in adult mouse-derived fibroblasts. Finally, we investigated the mechanisms of increased proliferation, reduced senescence, and inhibition of cell death and growth arrest in fibroblasts by collagen complexes.

Materials and Methods

Animal ethics

All animal experiments were approved and performed in accordance with the guidelines of the Konkuk University Animal Care and Experimentation committee (IACUC approval number: KU11035). The mice were housed in wire cages at 22 ± 1 C under a 12 h light–dark cycle with 70% humidity. Mice were fed a standard diet *ad libitum*.

Experimental designs

To examine the beneficial effects of the rejuvenation of skin fibroblasts obtained from adult mice, we produced transgenic mice harboring the Yamanaka four factors, and then made double transgenic mice harboring both the four Yamanaka factors and *Oct3/4-GFP* genes by mating with Oct3/4-GFP mice. Adult (A, over 1 year old) and young (Y, 1 month old) mouse-derived fibroblasts were obtained from these double transgenic mice to avoid transfection variability, respectively. A-fibroblasts cultured on dishes coated with collagen complexes were designated as "Ac-fibroblasts". Next, rejuvenation effects of Ac-fibroblasts were checked using the senescence-associated beta-galactosidase (SA-βgal) assay, cell proliferation assay, TUNEL assay, and *p16* mRNA expression analysis. Finally, the efficiency of reprogramming of from adult mouse-derived fibroblasts with or without treatment of collagen complexes was examined by counting the number of iPS cell colonies.

pTET-CKOS plasmid construction

c-Myc-2A, *Klf4-2A*, and *Oct4-2A* PCR products containing the 2A sequences of the foot-and-mouth disease virus (5′-aga gcc gag ggc agg gga agt ctt cta aca tgc ggg gac gtg gag gaa aat ccc ggg ccc-3′ encoded 2A peptides, RAEGRGSLLTCGDVEENPGP) were inserted into pTracer-EF/V6-His A vector (CLONTECH, Mountain View, CA, USA) with appropriate restriction enzymes to generate pMyc-2A, pKlf4-2A, and pOct4-2A vectors using complementary DNA derived from pig blastocyst or embryonic tissues and gene-specific primers: *c-Myc*-F (*Kpn*I-*Bam*HI), 5′-ggt acc gga tcc ATG CCC CTC AAC GTC AGC TTC A-3′, *c-Myc*-R (SpeI), 5′-act agt GGG CCC GGG ATT TTC CTC CAC GTC CCC GCA TGT TAG AA-3′, and c-Myc-2A-R (SpeI): 5′-act agt GGG CCC GGG ATT TTC CTC CAC GTC CCC GCA TGT TAG AAG ACT TCC CCT GCC CTC GGC TCT TGG GCA AGA GTT CCG TAG CTG-3′, for pMyc-2A; *Klf4*-F (SpeI), 5′-act agt ATG GCT GTC AGC GAC GCA CT-3′, *Klf4*-R (*Eco*RI), 5′-gaa ttc GGG CCC GGG ATT TTC CTC CAC

GTC CCC GCA TGT TAG AA-3′, and Klf4-2A-R(*Eco*RI): 5′-gaa ttc GGG CCC GGG ATT TTC CTC CAC GTC CCC GCA TGT TAG AAG ACT TCC CCT GCC CTC GGC TCT AAA ATG CCT CTT CAT GTG TAA GCC-3′, for pKlf4-2A; and, *Oct4*-F (*Eco*RI), 5′-gaa ttc ATG GCG GGA CAC CTG GCT T-3′, *Oct4*-R (*Eco*RV), 5′-gat atc GGG CCC GGG ATT TTC CTC CAC GTC CCC GCA TGT TAG AA-3′, and Otc4-2A-R (*Eco*RV), 5′-gat atc GGG CCC GGG ATT TTC CTC CAC GTC CCC GCA TGT TAG AAG ACT TCC CCT GCC CTC GGC TCT GTT TGA ATG CAT GGG GGA GCC-3′, for pOct4-2A. pSox2 vector containing a unique termination codon was constructed using gene-specific primers: *Sox2*-F (*Eco*RV), 5′-gat atc ATG TAC AAC ATG ATG GAG ACG GAG-3′, and *Sox2*-R(*Not*I), 5′-gcg gcc gcT CAC ATG TGA GAG AGA GGC AGT-3′. To construct pc-Myc(2A)-Klf4(2A)-Oct4(2A)-Sox2, a 1416 bp Klf4-2A fragment digested with SpeI and *Eco*RI restriction enzymes from pKlf4-2A vector was ligated into pMyc-2A to generate pc-Myc(2A)-Klf4(2A), 1140 bp Oct4-2A fragment digested with *Eco*RI and *Eco*RV restriction enzymes from pOct4-2A vector was ligated into pc-Myc(2A)-Klf4(2A) to generate pc-Myc(2A)-Klf4(2A)-Oct4(2A), and 954 bp Sox2 fragment having the translation termination codon in the same reading frame digested with *Eco*RV and *Not*I restriction enzymes was ligated into pc-Myc(2A)-Klf4(2A)-Oct4(2A) to generate pc-Myc(2A)-Klf4(2A)-Oct4(2A)-Sox2 vector successively. These cDNA-2A-cDNA-2A-cDNA-2A-cDNA STOP constructs were finally inserted into the *Bam*HI and *Xho*I sites of pTet-GRTW to generate a pTet-CKOS plasmid (Supplementary Fig. 1A), a retrovirus vector plasmid designed to express four transcription factor genes (*c-Myc*, *Klf4*, *Sox2*, and *Oct3/4*) under the control of the tetracycline promoter, which was constructed by modification of the pGWRT plasmid described previously [19, 20]. Detailed information on the pCKOS plasmid is provided in Supplementary Fig. 1.

Generation of heterozygous and homozygous transgenic mice

Transgenic mice were produced as described previously [21]. For generation of homozygous transgenic mice, heterozygous male and female B6D2F-1 transgenic mice were mated. Heterozygous and homozygous transgenic mice were confirmed by PCR. The primers used are given in Supplementary Table 1 (online only).

Extraction of collagen complexes and determination of optimal concentration

The tissues were cut into smaller pieces and suspended in 30 volumes of 0.5 mol/l acetic acid containing 2% pepsin at 4 C for 48 h. The supernatants of the extracted solutions were collected by centrifugation at $10,000 \times g$ for 15 min at 4 C to remove insoluble substances, and then salted out using 0.7 mol/l NaCl. The resultant precipitate was collected by centrifugation, dissolved in 0.5 mol/l acetic acid, and dialyzed against 0.1 mol/l acetic acid at 4 C for three days. The collagen concentrations were determined indirectly from the hydroxyproline concentrations, which were analyzed using the method of Bergman and Loxyler [22]. To determine the appropriate concentrations, we examined the effect of collagen complexes at various concentrations (10, 25, 50 and 100 μg/ml) on adult mouse-derived fibroblast proliferation using an SA-βgal assay. Based on these experimental results, we determined that 50 μg/ml was the most appropriate concentration for our experiments.

Cell proliferation assay

In this study, we prepared mouse fibroblasts from skin tissue of young (1 month old; Y-fibroblasts) and adult (1 year old; A-fibroblasts) double transgenic mice with the four Yamanaka factor genes under the control of the TREmCMV promoter and the GFP gene under the control of the Oct3/4 promoter (OG). Fibroblasts were cultured in Dulbecco's modified Eagle medium (DMEM; Invitrogen, Grand Island, NY, USA) containing 10% fetal bovine serum (Invitrogen). Cell proliferation was determined using a colorimetric immunoassay for the quantification of cell proliferation by measuring 5′-Bromo 2′-deoxyuridine (BrdU) incorporation during DNA synthesis. The BrdU assay was performed according to the protocol provided by the manufacturer (Roche Applied Science, Indianapolis, IN, USA).

Senescence-associated beta-galactosidase (SA-βgal) assay

Cytochemical detection of SA-β gal activity requires incubation of fixed Y-, Ac-, and A-fibroblasts with the chromogenic β-gal substrate X-gal in a buffer at pH 6.0. A blue color develops after 12–16 h of incubation at 37°C. After staining, the cells were washed with phosphate-buffered saline (PBS) and viewed by bright-field or phase contrast microscopy. The proportion of cells positive for SA-βgal activity was determined by counting the number of blue cells in the total population.

Western blot analysis

Cells in a semi-confluent state were lysed with M-PER (Thermo Scientific, Pittsburg, PA, USA) supplemented with protease inhibitor cocktail (Roche). Ten microliters of the cell lysate was separated by electrophoresis on 8% SDS-polyacrylamide gels, and then transferred to a nitrocellulose membrane (Millipore, Billerica MA, USA). Each membrane was washed with Tris-buffered saline Tween-20 (TBST), which consisted of 10 mM Tris–HCl (pH 7.6), 150 mM NaCl, and 0.05% Tween-20, blocked with 5% skim milk for 1 h at room temperature, and probed with the following primary antibodies: Collagen III (Abcam Ab7778), Collagen IV (Abcam Ab6586), Collagen II (Abcam Ab34712), Collagen I (Abcam Ab34710), Integrin α2 (Abcam 112310), Notch (Abcam 52301), Bmi (Abcam 38295), Gli (Abcam ab49314), PCNA (Abcam ab19166), p16 (Abcam ab51243), cyclin D1 (Abcam ab7958), pRb (Abcam ab47763) and β-actin (Abcam ab8227). Signals were detected with anti-mouse IgG-HRP (1:3000, Abcam) or anti-rabbit IgG-HRP (1:2000, Abcam). Bands were visualized with an enhanced chemiluminescence kit (Thermo Scientific, Pittsburg, PA, USA).

Mouse iPS cell derivation

Fibroblasts were cultured in DMEM containing 10% fetal bovine serum (Invitrogen). One hundred thousand cells per well were plated on an MEF feeder layered in six-well plates. Forty-eight hours later, fibroblast medium was replaced with mouse ESC media supplemented with doxycycline (2 μg/ml). No GFP+ growth was observed in cultures lacking Dox. GFP+ iPS cell formation was scored four weeks after Dox induction. Representative experiments were performed in triplicate.

Flow cytometry

Cells were trypsinized, washed once in PBS, and resuspended in fluorescence-activated cell sorting (FACS) buffer (PBS + 5% FBS). One million cells were resuspended in PBA (phosphate-buffered salt solution with 0.1% BSA and 0.01% sodium azide) with 2 mg/ml propidium iodide. Flow cytometric analysis was performed using a flow cytometer (BD Bioscience, Franklin Lakes, NJ, USA).

Real-time quantitative reverse transcriptase PCR (RT-qPCR)

Total mRNA was isolated by guanidinium thiocyanate-phenol-chloroform extraction (TRIzol, Qiagen, Hilden, Germany) and reverse transcribed using easy reverse transcriptase (Qiagen) according to the manufacturer's protocol. PCR amplification of different genes was performed using 2X easy SuperMix (Thermo). The primers used are given in Supplementary Table 1.

Immunofluorescence

Cells were fixed with 4% formaldehyde in PBS at room temperature for 20–30 min. After fixation, cells were treated with 0.4% Triton X-100 in PBS for 5 min at room temperature. After blocking with 10% FBS for 30 min, cells were incubated at room temperature at 4 C overnight with a primary antibody, followed by washing in PBS, and incubation at room temperature for 1 h with the corresponding secondary antibody. Nuclei were stained with 4′6-diamidino-2-phenylindole (Invitrogen). For immunofluorescence, the primary antibodies used were as follows: Albumin (Abcam ab112971), α-SMA (Abcam ab5694), NSE (Abcam ab53025), SSEA-1 (Millipore FCMAB117P), Oct4 (Abcam ab19857), Sox2 (Abcam ab97957), Nanog (Abcam ab80892), and c-myc (Abcam ab32072). The secondary antibody (Abcam) was rhodamine-labeled donkey anti-rabbit IgG.

Combined bisulfate restriction analysis and bisulfate sequencing analysis

Genomic DNA was treated with sodium bisulfate to convert all un-methylated cytosine to uracil residues using an EZ DNA Methylation Kit (Zymo Research, Orange, CA, USA), according to the manufacturer's protocol and our previous report [23]. Using this template, we amplified the indicated differentially methylated regions (DMRs) by PCR with the specific primers (5′-TTATTTGTTGAAATTGTTGTTTTTTTT-3′ and 5′-AAATCTAACTACCAAAATCCCCC-3′ for PCNA; 5′-GGTTTTTTAGAGGATGGTTGAGTG-3′ and 5′-TCCACAATA-TACCATCCCTC-3′ for Oct4. The PCR products were digested with the indicated restriction enzyme (Aci 1), which had recognition sequences containing CpG in the original unconverted DNA. The intensity of the digested bands was assessed using ImageJ (http://rsbweb.nih.gov/ij/).

Teratoma formation

Approximately 1×10^6 reprogrammed cells were injected subcutaneously or into the testis of 5-week-old immunodeficient nude mice to evaluate teratoma formation. For controls, mouse ES cells were injected into some of the mice. After 5–6 weeks, teratomas were fixed in paraformaldehyde, embedded in paraffin wax and sectioned for histology.

Statistical analysis

All results are presented as the mean ± standard deviation (SD). Statistical analysis was completed using the Student's *t* test, one-way

analysis of variance (ANOVA), Bonferroni correction and Tukey tests using Statistical Analysis System (SAS. 9.13 package). A P-value of < 0.05 was considered significant.

Results

Generation of transgenic mice expressing tetracycline-inducible stemness factor genes

pTet-CKOS, a retrovirus vector plasmid designed to express the stemness factors CKOS (*c-Myc*, *Klf4*, *Oct3/4*, and *Sox2*) genes the under the control of the *tetracycline* promoter gene, was constructed via multiple steps of cloning as described in Fig. 1A. The pTet-CKOS vector contained a polycistronic cassette CKOS with 2A peptide sequences to yield distinct polypeptides. A retrovirus vector was designed to express CKOS and rtTA (reverse tetracycline-controlled transactivator) under the control of the tetracycline-inducible promoter and *CMV* promoter genes, respectively. The transcription of CKOS was driven by minimal cytomegalovirus promoter in the tetracycline-response element sequence (TREmCMV). The pTet-CKOS vectors were injected into the pronucleus using manipulators. A total of 280 microinjected two-cell embryos were transferred into nine recipient mice. Of these, five recipients developed to term and naturally delivered 42 mice. To confirm that these were transgenic mice, we designed PCR primers to amplify and sequence the genomic DNA flanking each *CKOS* genes. The results showed that 8 of 42 mice were transgenic mice (Fig. 1B). Eight founder mice presented normal phenotypes, as the transgene is not active without the presence of transactivator expression. Furthermore, all transgenic lines produced their pups normally. As shown in Fig. 1C, fibroblasts derived from transgenic mice showed, after Dox induction, increased expression of the Yamanaka stemness factors, indicating that the vector worked well.

Mouse tail-derived total collagen complexes promote cell proliferation and ablate effectors of cellular senescence

We isolated total collagen complexes from the tails of young and/or adult mice. The total collagen levels, assessed using the Sircol Collagen Assay [22], were 11.7 mg/ml for whole young mouse tails and 0.96 mg/ml for aged mouse tails. Since there was no difference in the capacity of the two preparations to rejuvenate fibroblasts from adult mice, we used collagen derived from the tails of young mice for further studies (Supplementary Fig. 2A: online only). In our preparation of collagen complexes, the amount of the four collagen components ranged from 30% for type I collagen, to less than half of that for type IV collagen (Supplementary Fig. 2B and C).

Mouse fibroblasts were prepared from young (1 month old; Y-fibroblasts) and adult (1 year old; A-fibroblasts) double transgenic mice. These transgenic mouse–derived cells contained the four transcription factor genes under the control of the *TREmCMV* promoter and the *green fluorescent protein (GFP)* gene under the control of *Oct3/4* promoter (OG) gene. Cells derived from young and adult animals were cultured in the absence (Y- and A-fibroblasts) or presence (Ac-fibroblasts) of a collagen complex coating on the culture dishes.

To evaluate cellular senescence in the fibroblast populations, we stained for SA-β gal, a common marker of senescence (Fig. 2A). A-fibroblast cultures had more SA-β gal-positive cells ($32.1 \pm 1.75\%$

vs. $8.98 \pm 1.06\%$) than those of Y- and Ac-fibroblasts ($4.6 \pm 0.72\%$ *vs.* $8.98 \pm 1.06\%$). To determine if the decline in numbers of SA-β gal-positive cells occurred with cell cycle arrest, we measured the proliferation index in Y- and A-fibroblasts. A BrdU incorporation assay showed that Ac-fibroblasts had a higher proliferation index (2.7 ± 0.14) than A-fibroblasts (1.8 ± 0.08) (Fig. 2B). Together, these experiments indicated that collagen complexes present as an extracellular matrix can modulate the growth of fibroblasts.

To identify the component(s) of the collagen complex that prevents cellular senescence, we examined SA-β-galactosidase positivity in A-fibroblasts cultured with different types of collagen. Commercially available dishes coated with collagen types I, II, III, and IV were compared with dishes coated with collagen complexes (Ac, total) (Fig. 2C). Each type of collagen significantly reduced the number of Sa-β gal-positive cells in A-fibroblasts, with the collagen complexes (total; $8.9 \pm 1.06\%$) and collagen type I preparation ($10.96 \pm 1.12\%$) being more potent than preparations of collagen type II and III (24.5 ± 1.75 *vs.* 27.4 ± 0.72; $P < 0.05$). This suggests that the collagen complex resets rejuvenation of A-fibroblasts.

Rejuvenation of fibroblasts, without dedifferentiation, by treatment with collagen complexes is induced by an α2β1 integrin-dependent Bmi-1 pathway

To address whether treatment with collagen complexes blocks apoptosis in A-fibroblasts, apoptosis in Y-, Ac-, and A-fibroblasts was analyzed by flow cytometry. Flow cytometric analysis using Annexin V-FITC staining showed that *in vitro* culture of A-fibroblasts caused a significant increase in the percentage of apoptotic cells ($19.9 \pm 3.2\%$) (Fig. 2D). In contrast, a marked decrease ($11.9 \pm 2.8\%$) in the frequency of Annexin V-positive cells was observed in Ac-fibroblasts. The survival rate of Ac-fibroblasts reached Y-fibroblast cell levels after five days of culture with collagen complexes.

To study the molecular mechanism underlying the rejuvenation of Ac-fibroblasts by total collagen complexes, protein expression levels of the integrin pathway, specifically integrin α2, Notch, Gli-1, and Bmi-1, were examined by Western blot analysis (Fig. 3A). Ac-fibroblasts showed higher levels of integrin α2, Notch, Gli-1, and Bmi-1 than A-fibroblasts, and these increased levels matched those in Y-fibroblasts. Similarly, on Day 5 of culture with collagen complexes, the levels of cyclinD1, ppRB, and PCNA protein were higher in Ac-fibroblasts than in A-fibroblasts (Fig. 3B). Five days after collagen complex treatment, Ac-fibroblasts expressed mRNA levels of *p15*, *p16*, and *p21* that were similar to Y-fibroblasts. Of note, *p19* and *p53* mRNAs expressions were significantly increased compared with those in Y-fibroblasts, but their expressions were significantly decreased compared with those in A-fibroblasts. This is consistent with the collagen complexes inducing increases in cyclin D1, PCNA, and ppRB protein expression by suppressing p16 protein levels in A-fibroblasts. Although the *PCNA* gene promoter region exhibited more hypomethylation in old age-derived fibroblasts cultured in the presence of collagen complexes for 5 dyas than in Y age-derived fibroblasts, the protein level was similar between them. (Supplementary Fig. 3B: online only). Therefore, Ac-fibroblast proliferation is regulated by epigenetic modification. Taken together, rejuvenation of adult age-derived somatic cells is likely to be regulated, in part, through an α2β1 integrin-dependent Bmi-1 pathway (Fig. 3D).
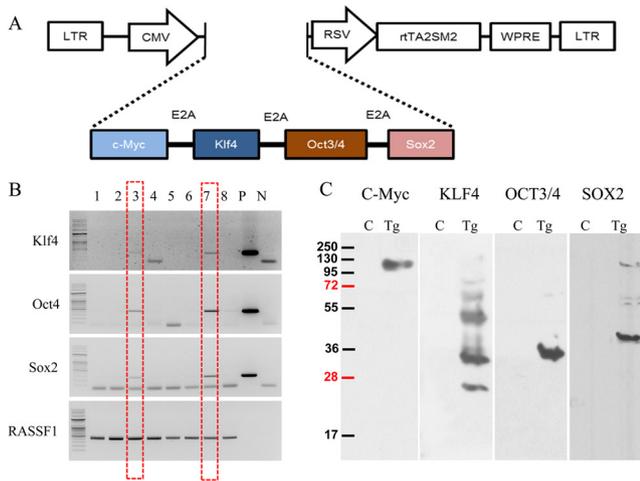
Fig. 1. Construction of the retroviral vector for generation of transgenic mice. (A) The retrovirus vector was designed to express the four stemness factors by tetracycline-mediated induction. For further details, see the Methods section. (B) Confirmation of transgenic mice using four-factor PCR. Red dotted lines indicate transgenic mice. (C) Western blotting analysis of the four stemness factors with tetracycline-mediated induction in control and transgenic mouse-derived fibroblasts. Fibroblasts were isolated and cultured by adding doxycycline for 10 days and then subjected to Western blot analysis using each antibody.
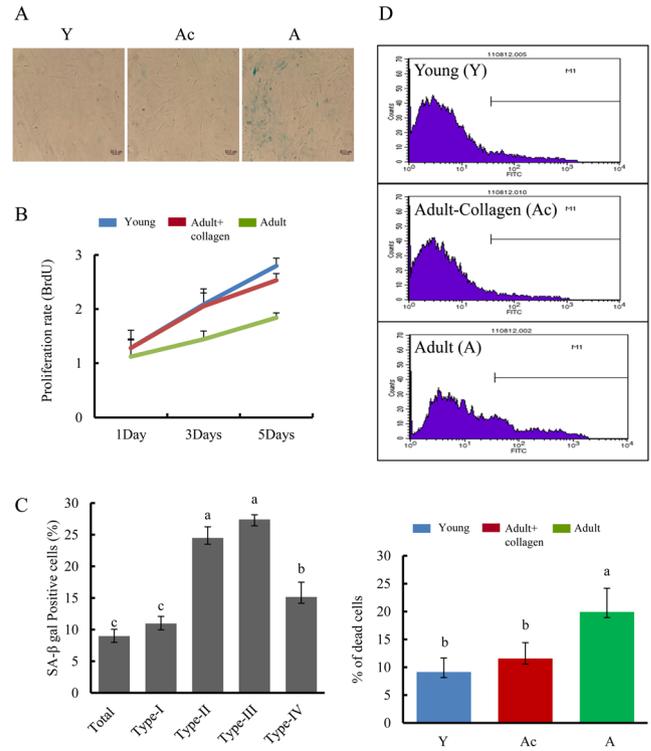

Fig. 3. α2β1 integrin-dependent Bmi-1 regulation analysis in adult fibroblasts cultured with collagen complexes. (A) Western blot analysis in Y-, Ac-, and A-fibroblasts. (B) Western blot analysis of cell cycle regulatory proteins in Y-, Ac-, and A-fibroblasts. (C) RT-qPCR analysis of expression of Ink4/Arf tumor suppressor locus genes in Y-, Ac-, and A-fibroblasts. RT-qPCR was normalized to GAPDH levels. Groups marked with different letters (a–c) are significantly different from each other at P < 0.05. (D) Schema for the rejuvenation in aged fibroblasts on dishes coated with collagen complexes.

Fig. 2. Effects on both of senescence and apoptosis of collagen complexes. A) Senescence-associated β-galactosidase staining (blue) in Y-, Ac-, and A-fibroblasts. Magnification, × 200. B) Cell proliferation assay. Data are means ± SEM of three experiments performed in triplicate with p values < 0.05. C) Senescence-associated β-galactosidase staining in A-fibroblasts according to collagen types. D) Determination of apoptotic Y-, Ac-, and A- fibroblasts by FACS analysis. (down) Data were obtained from three independent experiments (means ± SD; lower panel; P < 0.05). Groups marked with different letters (a–c) are significantly different from each other at P < 0.05.
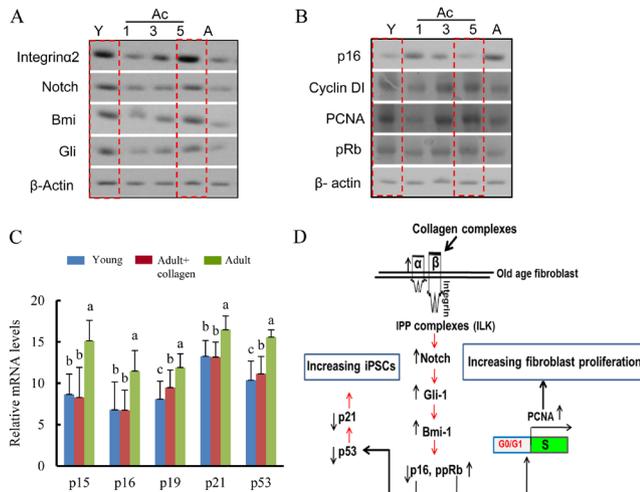
Collagen complex treatment of adult mouse-derived fibroblasts generated iPS cells with high efficacy due to low Ink4a/Arf locus gene expression

We used homozygous transgenic mice harboring the four pluripotency-associated factors and *Oct3/4-GFP* genes to avoid transfection variability. To evaluate the dedifferentiation capacity of Y-, Ac-, and A-fibroblasts, cells were incubated in serum containing medium for 1, 3, and 5 days and then analyzed for expression of the genes of the *Ink4a/Arf* locus, such as CDK inhibitors, *p15*, *p16^Ink4a*, *p19^Arf*, and *p21*, which have been reported to contribute to aging of both hematopoietic stem cells and neuronal stem cells [24, 25], using quantitative real-time RT-qPCR analysis. The mRNA expression of *p15* (8.6 ± 2.4 and 8.2 ± 3.6), *p16^Ink4a* (6.7 ± 2.4 and 6.7 ± 2.1), *p19^Arf* (9.4 ± 2.1 and 8.08 ± 2.1), *p21* (13.1 ± 1.8 and 13.2 ± 2.3), and *p53* (11.1 ± 2.0 and 10.3 ± 2.3) in Ac- and Y-fibroblasts was lower than that in A-fibroblasts (*p15*, 15.16 ± 2.4; *p16^Ink4a*, 11.47 ± 2.4; *p19^Arf*, 11.9 ± 1.6; *p21*, 16.4 ± 1.6; and *p53*, 15.5 ± 0.83) (Fig. 3C). In this study, *Akt* (3.7 ± 0.12 and 4.14 ± 0.55), *Src* (5.2 ± 0.12 and 5.67 ± 0.07), *Map2K1* (4.73 ± 0.25 and 4.5 ± 0.45), and *mTOR*
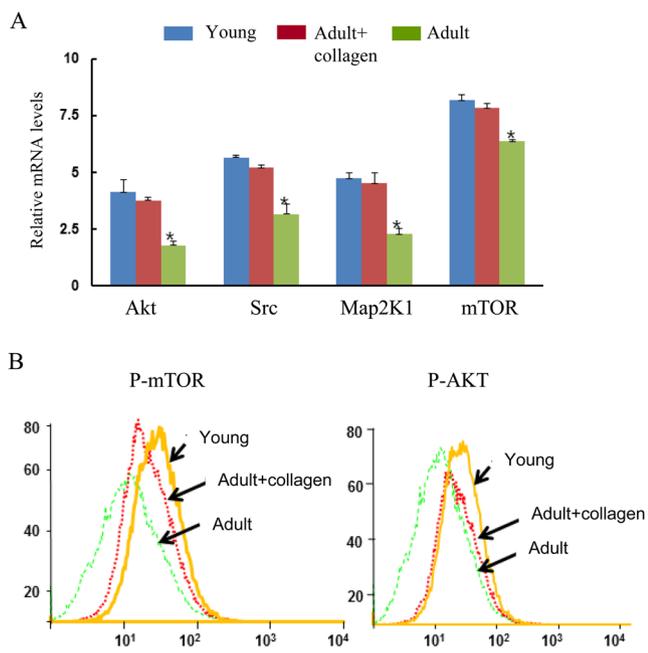
A

B

Fig. 4. Real-time RT-qPCR and flow cytometry analysis of AKT/mTOR-related gene expression. A) Akt, Src, Map2K1, and mROR mRNA expression in Y-, Ac-, and A-derived fibroblasts. Gene expression was normalized using a GAPDH housekeeping gene. B) Comparison of p-Akt and p-mTOR expression using flow cytometry in Y-, Ac-, and A-derived fibroblasts.

(7.82 ± 0.19 and 8.16 ± 0.23) expression in Ac- and Y-fibroblasts was significantly higher than in A-fibroblasts (1.7 ± 0.17, 3.17 ± 0.43, 2.29 ± 0.22, and 6.37 ± 0.07), respectively (Fig. 4A). In addition, flow cytometry analysis demonstrated that collagen treatment of adult mouse-derived fibroblasts (Ac-fibroblast) resulted in higher p-Akt and p-mTOR expression than in A-fibroblasts (Fig. 4B). Considering
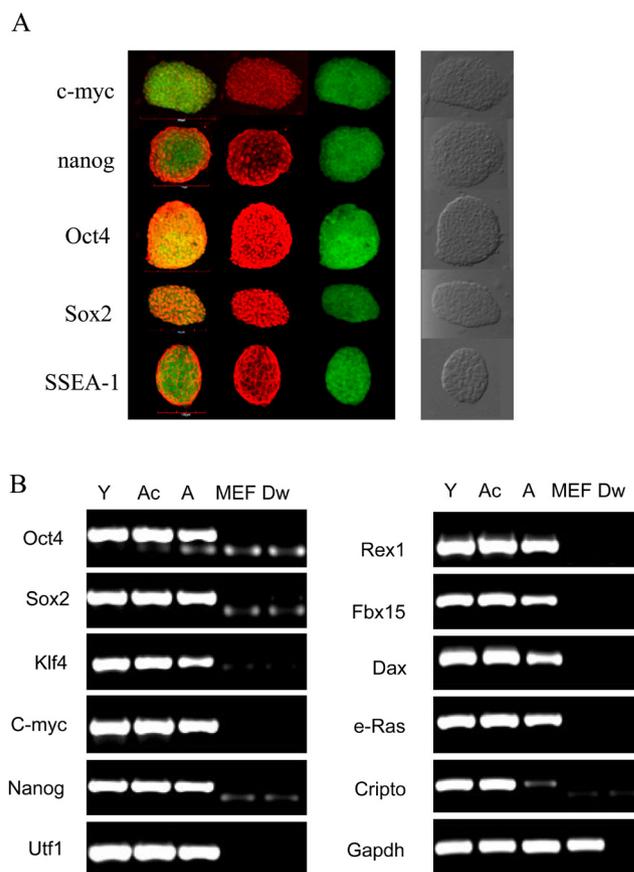
A

B

Fig. 5. Generation of iPS cells. A) Immunostaining analysis using pluripotency markers such as c-myc, Nanog, Oct3/4, Sox2, and SSEA-1. Nuclei were stained with DAPI. B) Pluripotency marker expression. Primers used for *Oct4*, *Sox2*, *Klf4*, *c-Myc*, *Nanog*, *Utf1*, *Rex1*, *Fbx15*, *Dax*, *e-Ras*, and *Cripto* specifically detected the mRNA transcripts.
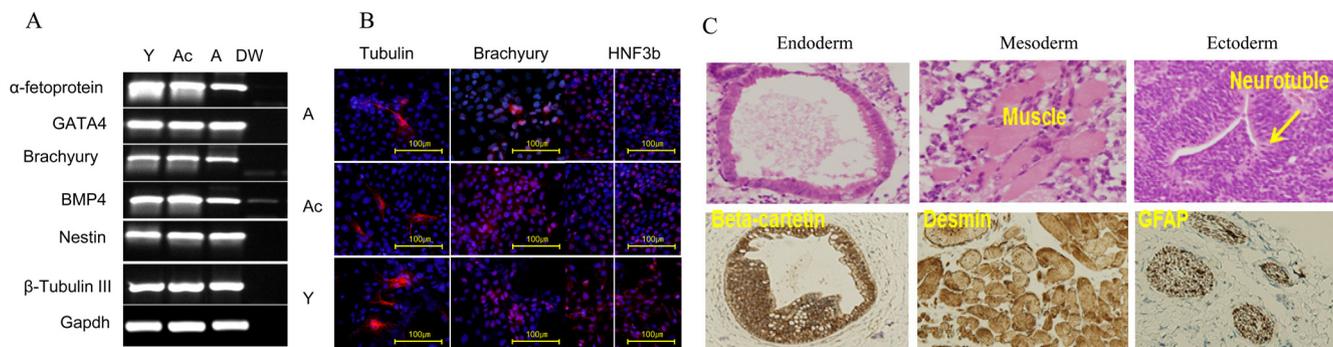
A

B

C

Fig. 6. Differentiation of iPS cells *in vitro* and *in vivo*. A) RT-PCR analysis of differentiation markers for the three germ layers (endoderm, *GATA4* and *α-fetoprotein*; mesoderm, *brachyury* and *GATA2*; and ectoderm, *NESTIN* and *βIII-tubulin*). Of note, a faint signal of BMP4 RT-PCR product in distilled water may be caused by flowing during application of electrophoresis to an RT-PCR product derived from A-derived iPS cells. Y, Ac, A and DW indicate Y-, Ac-, A-derived iPS cells, and distilled water, respectively. B) Immunocytochemical analysis of representative iPS cell lines during *in vitro* differentiation using three germ layer markers (ectoderm, tubulin; mesoderm, brachyury; endoderm, HNF3b). C) Teratoma formation analysis. Histological sections were examined with H&E staining and immunohistochemistry. Endodermal derivatives, epithelia, expressed a high level of beta-catenin. Mesodermal derivatives were exemplified by striated muscle and smooth muscle (middle). Tissues of ectodermal lineage, including the neural epithelium, expressed glial fibrillary acidic protein (GFAP).

that Akt promotes the expression of cyclin D1 and c-Myc through the PI3K/Akt-mammalian target of rapamycin (mTOR) pathway and suppresses the expression of *p15*, *p16*, *p19* and *p21* mRNAs, these findings suggest that the downregulation of genes of the Ink4a/Arf locus may be caused by PI3K/Akt overexpression.

Autophagy in the cultures was also assessed. To normalize the RT-qPCR reaction efficiency, *GAPDH* was used as an internal standard. After normalization, the concentrations of autophagy-specific mRNAs in Ac-fibroblasts were equal to those of Y-fibroblasts, but significantly increased compared with those of A-fibroblasts (Supplementary Fig. 4: online only). These observations indicate that the prevention of cellular senescence from aged cells is closely matched with upregulation of autophagy-related gene expression.

Next, we examined the kinetics of reprogramming Y-, Ac-, and A-fibroblasts exposed to Dox. No colonies were detected on plates that were not treated with Dox or were treated for less than 10 days (data not shown). At 20 or 25 days after initial Dox addition, colonies resembling mESCs, i.e., those with a high nucleus-to-cytoplasmic ratio, prominent nucleoli, and well defined phase-bright borders, were picked and expanded. Reprogramming efficiency was defined as the number of GFP-positive colonies per 10,000 Y-, Ac, and A-fibroblasts seeded. Significantly higher reprogramming efficiency was observed for Y- and Ac-fibroblasts ($1.01 \pm 0.05\%$ and $0.82 \pm 0.05\%$) than for A-fibroblasts ($0.22 \pm 0.02\%$).

Analysis of pluripotency markers revealed that expression of the exogenous *Oct4*, *Sox2*, *Klf4*, and *c-Myc* genes in the Y-, A-, and Ac-iPS cells was similar. Additional ES markers (Nanog, Utf1, Rex1, Fbx15, Dax, e-Ras, and Cripto) were also detected at similar levels in Y-, A-, and Ac-iPS cells (Fig. 5B), compared with those of stained with antibodies against Oct3/4, Klf4, Sox2, c-Myc, Nanog and SSEA-1 (Fig. 5A). Bisulfite genomic sequencing analysis revealed further similarities among Y-, Ac-, and A-iPS cells. The promoter region of the *Oct3/4* gene in iPS cells was highly demethylated (1.9%; 2/105), whereas the CpG dinucleotides of *Oct3/4* promoter gene regions in fibroblasts were highly methylated (75.7%; 78/103) (Supplementary Fig. 3C).

We executed spontaneous differentiation of Y-, Ac-, and A-iPS cells to determine their pluripotency and/or capability to dedifferentiate into fully rejuvenated cells. Embryoid body (EB) formation was performed by culturing three iPS cells in differentiation media on low-attachment plates. We confirmed their differentiation into diverse cell types of three germ layers by checking the expression of specific markers for ectodermal (Nestin and β-tubulin III), endodermal (α-fetoprotein and GATA4), and mesodermal (Brachyury and BMP4) lineages by RT-PCR analysis or *in vitro* differentiation (Fig. 6A and B). Next, we injected iPS cells into the testis of nude mice. The resulting teratomas contained unorganized and mixed types of tissues, and striated muscle (mesoderm) tissues were distributed randomly, forming many islands throughout (Fig. 6C). They included secretory epithelia (i.e., epithelium lined with goblet cells, endoderm) and neural epithelium (ectoderm), indicating that the iPS cells were cells are functionally pluripotent.

Discussion

The present study provides evidence that biologically active

collagen complexes, prepared from the tails of young mice, reduce cellular senescence in fibroblast cultures derived from aged mice. This was demonstrated by measuring the frequency of SA-β gal positivity, a marker of senescence. A-fibroblast preparations had more SA-β gal-positive cells than Ac- or Y-fibroblast preparations (Fig. 2A). Proliferative capacity was also enhanced by the collagen complexes, as measured by BrdU incorporation assays. Ac-fibroblasts had a higher proliferation index than A-fibroblasts (Fig. 2B), which was consistent with the results of a previous study [26].

To gain insight into the mechanism underlining the rejuvenation of Ac-fibroblasts, we examined the expression of Integrin α2 and the integrin-associated proteins Notch, Gli-1, and Bmi-1, which are located downstream of α2β1 integrin in the Bmi-1 pathway. Ac-fibroblasts highly expressed these proteins (Fig. 3A). Furthermore, the total collagen complex preparation and commercial collagen type I alone induced similar effects (Fig. 2C). Previous studies reported that embryonic stem cells (ESCs) cultured on collagen type I had an increased proliferative capacity dependent upon Notch signaling [27–30]. The present study, like a previous study [26], suggested that type I collagen among collagen complexes rescued proliferation capacity in the A-fibroblasts.

A recent study [31] reported that inhibition of autophagy would increase the rate of apoptosis, which is another p53-regulated response to the overexpression of exogenous Yamanaka transcription factors that markedly decreases the efficiency of reprogramming. If autophagy is induced during the process of cellular senescence, it provides a pivotal roadblock during reprogramming of cells into iPS cells. However, it is unclear whether autophagy imposed by collagen complexes can significantly enhance iPS cell generation or not. As shown in Supplementary Fig. 4, expression of autophagy-specific mRNAs in Ac- and Y-fibroblasts was significantly higher than that in A-fibroblasts cells. Furthermore, our results showed that the autophagy-specific mRNA reduction in A-fibroblasts is coincident with the deactivation of the integrin α2-dependent Gli-1 pathway. We found that expression of genes of the Ink4a/Arf locus (CDK inhibitors), such as *p15*, *p16*[Ink4a], *p19*[Arf] and *p21*, were lower in Ac-fibroblasts than in A-fibroblasts (Fig. 3C). As shown in Fig. 4, *Akt* gene expression was higher in Ac-fibroblasts than in A-fibroblasts. As a result of *Akt* gene overexpression, *Map2K1*, *Src*, and *mTOR* gene expression, which is located downstream of the *Akt* gene, was significantly higher in Ac-fibroblasts than in A-fibroblasts. This finding suggests that *Akt* also promotes the expression of *cyclinD1* and *c-Myc* through the PI3K/Akt-mammalian target of rapamycin (mTOR) pathway and suppresses the expression of *p15*, *p16*, *p19* and *p21*. The p16[Ink4a] protein inhibits cell cycle progression through repression of the CDK4/6 cyclin complexes and prevention of the phosphorylation of pRB, whereas the p19[Arf] protein plays important roles in the regulation of the p53 pathway [32]. It is well-known that the increase in cellular senescence with age is linked to physiological aging and is characterized by an irreversible cell cycle arrest, such as activation of the p53/p21 and p16/pRb pathway [33]. Previous studies have demonstrated that genetic inhibition of the Ink4/Arf locus has a profound positive effect on the efficiency of iPS cell generation, increasing the number of emerging colonies [34]. In addition, cell cycle-related gene promoter regions, such as PCNA, were extensively demethylated in Ac-fibroblasts compared with

A-fibroblasts (Supplementary Fig. 2). Taken together, the rejuvenation of fibroblasts derived from adult animals by treatment of collagen complexes might be caused by: 1) the activation of cell cycle promoting genes via the α2β1 integrin-dependent Bmi-1 pathway, 2) demethylation of cell cycle promoting genes, such as the PCNA gene promoter, 3) increased numbers of A-fibroblasts that reset to Y-fibroblast cell conditions, and 4) the blocking of apoptosis in A-fibroblasts.

In this study, iPS efficacy from Y- and Ac-fibroblasts was 40-50 times higher than that obtained in the original studies using a combination of *c-Myc*, *Klf-4*, *Sox-2*, and *Oct3/4* genes [2, 35]. Also, iPS colonies developed at efficiencies comparable to that in the original data from four factor transgenic mice [36]. A range of methods to improve reprogramming efficiency has been published, including: 1) use of chemicals that modify chromatin structure, such as valproic acid [37]; 2) use of 5-aza-cytidine [38]; 3) use of a combination of BIX and BayK [39]; 4) use of inhibitors of signaling pathways, such as TGF-β inhibitors [40] and a combination of MEK and GSK3 inhibitors [39, 41]; 5) use of antagonists of senescence, such as suppressors of p53 [42, 43]; 6) use of vitamin C [44]; 7) use of hypoxia [45] and 8) use of Cdh1 (E-cadherin) [46]. In this study, we demonstrated that A-fibroblasts grown on plates coated with collagen complexes for over five consecutive passages were more youthful, expanded at a higher rate, and exhibited lower spontaneous cell death than A-fibroblasts (Fig. 2).

Collagen, the most abundant ECM protein, has previously been ascribed key roles in the maintenance of stemness. The inhibition of endogenous collagen results in a gradual loss of ESC characteristics [16]. Also, another research group reported that solubilizing type I collagen enhanced the differentiation of rat bone marrow stem cells [47]. A recent study demonstrated that a collagen receptor, α2β1 integrin, regulates stem cell fate in human colorectal cancer cells [48], and type I collagen inhibits differentiation and promotes maintenance of a stem cell-like phenotype in human colorectal carcinoma cells and mESCs [18]. In conclusion, collagen complexes both stimulate proliferation and inhibit cell death and growth arrest in A-fibroblasts. Furthermore, the gene expression of CDK inhibitors, such as $p16^{Ink4a}$, $p19^{Arf}$, and $p21^{CIPI}$, was significantly downregulated in Ac-fibroblasts. As a result of these modifications, significantly higher inducible pluripotent stem (iPS) cell efficacy was observed for Y- and Ac-fibroblasts than for A-fibroblasts, indicating that collagen complex treatment might provide an alternative and safer source for producing iPS cells at high efficiency.

Acknowledgment

References

1. **Takahashi K, Yamanaka S.** Induction of pluripotent stem cells from mouse embryonic and adult fibroblast cultures by defined factors. *Cell* 2006; **126**: 663–676. [Medline] [CrossRef]

2. **Takahashi K, Tanabe K, Ohnuki M, Narita M, Ichisaka T, Tomoda K, Yamanaka S.** Induction of pluripotent stem cells from adult human fibroblasts by defined factors. *Cell* 2007; **131**: 861–872. [Medline] [CrossRef]

3. **Yu J, Vodyanik MA, Smuga-Otto K, Antosiewicz-Bourget J, Frane JL, Tian S, Nie J, Jonsdottir GA, Ruotti V, Stewart R, Slukvin II, Thomson JA.** Induced pluripotent stem cell lines derived from human somatic cells. *Science* 2007; **318**: 1917–1920. [Medline] [CrossRef]

4. **Lowry WE, Richter L, Yachechko R, Pyle AD, Tchieu J, Sridharan R, Clark AT, Plath K.** Generation of human induced pluripotent stem cells from dermal fibroblasts. *Proc Natl Acad Sci USA* 2008; **105**: 2883–2888. [Medline] [CrossRef]

5. **Nakagawa M, Koyanagi M, Tanabe K, Takahashi K, Ichisaka T, Aoi T, Okita K, Mochiduki Y, Takizawa N, Yamanaka S.** Generation of induced pluripotent stem cells without Myc from mouse and human fibroblasts. *Nat Biotechnol* 2008; **26**: 101–106. [Medline] [CrossRef]

6. **Park IH, Zhao R, West JA, Yabuuchi A, Huo H, Ince TA, Lerou PH, Lensch MW, Daley GQ.** Reprogramming of human somatic cells to pluripotency with defined factors. *Nature* 2008; **451**: 141–146. [Medline] [CrossRef]

7. **Okita K, Ichisaka T, Yamanaka S.** Generation of germline-competent induced pluripotent stem cells. *Nature* 2007; **448**: 313–317. [Medline] [CrossRef]

8. **Meissner A, Wernig M, Jaenisch R.** Direct reprogramming of genetically unmodified fibroblasts into pluripotent stem cells. *Nat Biotechnol* 2007; **25**: 1177–1181. [Medline] [CrossRef]

9. **Wernig M, Meissner A, Foreman R, Brambrink T, Ku M, Hochedlinger K, Bernstein BE, Jaenisch R.** In vitro reprogramming of fibroblasts into a pluripotent ES-cell-like state. *Nature* 2007; **448**: 318–324. [Medline] [CrossRef]

10. **Huang J, Chen T, Liu X, Jiang J, Li J, Li D, Liu XS, Li W, Kang J, Pei G.** More synergetic cooperation of Yamanaka factors in induced pluripotent stem cells than in embryonic stem cells. *Cell Res* 2009; **19**: 1127–1138. [Medline] [CrossRef]

11. **Hockemeyer D, Soldner F, Cook EG, Gao Q, Mitalipova M, Jaenisch R.** A drug-inducible system for direct reprogramming of human somatic cells to pluripotency. *Cell Stem Cell* 2008; **3**: 346–353. [Medline] [CrossRef]

12. **Banito A, Rashid ST, Acosta JC, Li S, Pereira CF, Geti I, Pinho S, Silva JC, Azuara V, Walsh M, Vallier L, Gil J.** Senescence impairs successful reprogramming to pluripotent stem cells. *Genes Dev* 2009; **23**: 2134–2139. [Medline] [CrossRef]

13. **Weaver VM, Petersen OW, Wang F, Larabell CA, Briand P, Damsky C, Bissell MJ.** Reversion of the malignant phenotype of human breast cells in three-dimensional culture and in vivo by integrin blocking antibodies. *J Cell Biol* 1997; **137**: 231–245. [Medline] [CrossRef]

14. **Lukashev ME, Werb Z.** ECM signalling: orchestrating cell behaviour and misbehaviour. *Trends Cell Biol* 1998; **8**: 437–441. [Medline] [CrossRef]

15. **Leitinger B, Hohenester E.** Mammalian collagen receptors. *Matrix Biol* 2007; **26**: 146–155. [Medline] [CrossRef]

16. **Chen SS, Fitzgerald W, Zimmerberg J, Kleinman HK, Margolis L.** Cell-cell and cell-extracellular matrix interactions regulate embryonic stem cell differentiation. *Stem Cells* 2007; **25**: 553–561. [Medline] [CrossRef]

17. **Kihara T, Hirose M, Oshima A, Ohgushi H.** Exogenous type I collagen facilitates osteogenic differentiation and acts as a substrate for mineralization of rat marrow mesenchymal stem cells in vitro. *Biochem Biophys Res Commun* 2006; **341**: 1029–1035. [Medline] [CrossRef]

18. **Suh HN, Han HJ.** Collagen I regulates the self-renewal of mouse embryonic stem cells through α2β1 integrin- and DDR1-dependent Bmi-1. *J Cell Physiol* 2011; **226**: 3422–3432. [Medline] [CrossRef]

19. **Choi BR, Koo BC, Ahn KS, Kwon MS, Kim JH, Cho SK, Kim KM, Kang JH, Shim H, Lee H, Uhm SJ, Lee HT, Kim T.** Tetracycline-inducible gene expression in nuclear transfer embryos derived from porcine fetal fibroblasts transformed with retrovirus vectors. *Mol Reprod Dev* 2006; **73**: 1221–1229. [Medline] [CrossRef]

20. **Zufferey R, Donello JE, Trono D, Hope TJ.** Woodchuck hepatitis virus posttranscriptional regulatory element enhances expression of transgenes delivered by retroviral vectors. *J Virol* 1999; **73**: 2886–2892. [Medline]

21. **Kwon DN, Choi YJ, Park JY, Cho SK, Kim MO, Lee HT, Kim JH.** Cloning and molecular dissection of the 8.8 kb pig uroplakin II promoter using transgenic mice and RT4 cells. *J Cell Biochem* 2006; **99**: 462–477. [Medline] [CrossRef]

22. **Bannister DW, Burns AB.** Adaptation of the Bergman and Loxley technique for hydroxyproline determination to the autoanalyzer and its use in determining plasma hydroxyproline in the domestic fowl. *Analyst (Lond)* 1970; **95**: 596–600. [Medline] [CrossRef]

23. **Cho SK, Kim JH, Park JY, Choi YJ, Bang JI, Hwang KC, Cho EJ, Sohn SH, Uhm SJ, Koo DB, Lee KK, Kim T, Kim JH.** Serial cloning of pigs by somatic cell nuclear transfer: restoration of phenotypic normality during serial cloning. *Dev Dyn* 2007; **236**: 3369–3382. [Medline] [CrossRef]

24. **Janzen V, Forkert R, Fleming HE, Saito Y, Waring MT, Dombkowski DM, Cheng T, DePinho RA, Sharpless NE, Scadden DT.** Stem-cell ageing modified by the cyclin-dependent kinase inhibitor p16INK4a. *Nature* 2006; **443**: 421–426. [Medline]

25. **Molofsky AV, Slutsky SG, Joseph NM, He S, Pardal R, Krishnamurthy J, Sharpless NE, Morrison SJ.** Increasing p16INK4a expression decreases forebrain progenitors and

neurogenesis during ageing. *Nature* 2006; **443**: 448–452. [Medline] [CrossRef]

26. **Volloch V, Kaplan D.** Matrix-mediated cellular rejuvenation. *Matrix Biol* 2002; **21**: 533–543. [Medline] [CrossRef]

27. **Hayashi Y, Furue MK, Okamoto T, Ohnuma K, Myoishi Y, Fukuhara Y, Abe T, Sato JD, Hata R, Asashima M.** Integrins regulate mouse embryonic stem cell self-renewal. *Stem Cells* 2007; **25**: 3005–3015. [Medline] [CrossRef]

28. **Heo JS, Lee MY, Han HJ.** Sonic hedgehog stimulates mouse embryonic stem cell proliferation by cooperation of Ca^{2+}/protein kinase C and epidermal growth factor receptor as well as Gli1 activation. *Stem Cells* 2007; **25**: 3069–3080. [Medline] [CrossRef]

29. **Mine T, Matsueda S, Gao H, Li Y, Wong KK, Peoples GE, Ferrone S, Ioannides CG.** Created Gli-1 duplex short-RNA (i-Gli-RNA) eliminates CD44 Hi progenitors of taxol-resistant ovarian cancer cells. *Oncol Rep* 2010; **23**: 1537–1543. [Medline]

30. **Wilschut KJ, Haagsman HP, Roelen BA.** Extracellular matrix components direct porcine muscle stem cell behavior. *Exp Cell Res* 2010; **316**: 341–352. [Medline] [CrossRef]

31. **Marión RM, Strati K, Li H, Murga M, Blanco R, Ortega S, Fernandez-Capetillo O, Serrano M, Blasco MA.** A p53-mediated DNA damage response limits reprogramming to ensure iPS cell genomic integrity. *Nature* 2009; **460**: 1149–1153. [Medline] [CrossRef]

32. **Stein GH, Drullinger LF, Soulard A, Dulić V.** Differential roles for cyclin-dependent kinase inhibitors p21 and p16 in the mechanisms of senescence and differentiation in human fibroblasts. *Mol Cell Biol* 1999; **19**: 2109–2117. [Medline]

33. **Lapasset L, Milhavet O, Prieur A, Besnard E, Babled A, Aït-Hamou N, Leschik J, Pellestor F, Ramirez JM, De Vos J, Lehmann S, Lemaitre JM.** Rejuvenating senescent and centenarian human cells by reprogramming through the pluripotent state. *Genes Dev* 2011; **25**: 2248–2253. [Medline] [CrossRef]

34. **Li H, Collado M, Villasante A, Strati K, Ortega S, Cañamero M, Blasco MA, Serrano M.** The Ink4/Arf locus is a barrier for iPS cell reprogramming. *Nature* 2009; **460**: 1136–1139. [Medline] [CrossRef]

35. **Takahashi K, Okita K, Nakagawa M, Yamanaka S.** Induction of pluripotent stem cells from fibroblast cultures. *Nat Protoc* 2007; **2**: 3081–3089. [Medline] [CrossRef]

36. **Markoulaki S, Hanna J, Beard C, Carey BW, Cheng AW, Lengner CJ, Dausman JA, Fu D, Gao Q, Wu S, Cassady JP, Jaenisch R.** Transgenic mice with defined combinations of drug-inducible reprogramming factors. *Nat Biotechnol* 2009; **27**: 169–171. [Medline] [CrossRef]

37. **Huangfu D, Osafune K, Maehr R, Guo W, Eijkelenboom A, Chen S, Muhlestein W, Melton DA.** Induction of pluripotent stem cells from primary human fibroblasts with only Oct4 and Sox2. *Nat Biotechnol* 2008; **26**: 1269–1275. [Medline] [CrossRef]

38. **Mikkelsen TS, Hanna J, Zhang X, Ku M, Wernig M, Schorderet P, Bernstein BE, Jaenisch R, Lander ES, Meissner A.** Dissecting direct reprogramming through integrative genomic analysis. *Nature* 2008; **454**: 49–55. [Medline] [CrossRef]

39. **Shi Y, Do JT, Desponts C, Hahm HS, Schöler HR, Ding S.** A combined chemical and genetic approach for the generation of induced pluripotent stem cells. *Cell Stem Cell* 2008; **2**: 525–528. [Medline] [CrossRef]

40. **Ichida JK, Blanchard J, Lam K, Son EY, Chung JE, Egli D, Loh KM, Carter AC, Di Giorgio FP, Koszka K, Huangfu D, Akutsu H, Liu DR, Rubin LL, Eggan K.** A small-molecule inhibitor of tgf-Beta signaling replaces sox2 in reprogramming by inducing nanog. *Cell Stem Cell* 2009; **5**: 491–503. [Medline] [CrossRef]

41. **Silva J, Barrandon O, Nichols J, Kawaguchi J, Theunissen TW, Smith A.** Promotion of reprogramming to ground state pluripotency by signal inhibition. *PLoS Biol* 2008; **6**: e253. [Medline] [CrossRef]

42. **Kawamura T, Suzuki J, Wang YV, Menendez S, Morera LB, Raya A, Wahl GM, Izpisúa Belmonte JC.** Linking the p53 tumour suppressor pathway to somatic cell reprogramming. *Nature* 2009; **460**: 1140–1144. [Medline] [CrossRef]

43. **Hong H, Takahashi K, Ichisaka T, Aoi T, Kanagawa O, Nakagawa M, Okita K, Yamanaka S.** Suppression of induced pluripotent stem cell generation by the p53-p21 pathway. *Nature* 2009; **460**: 1132–1135. [Medline] [CrossRef]

44. **Esteban MA, Wang T, Qin B, Yang J, Qin D, Cai J, Li W, Weng Z, Chen J, Ni S, Chen K, Li Y, Liu X, Xu J, Zhang S, Li F, He W, Labuda K, Song Y, Peterbauer A, Wolbank S, Redl H, Zhong M, Cai D, Zeng L, Pei D.** Vitamin C enhances the generation of mouse and human induced pluripotent stem cells. *Cell Stem Cell* 2010; **6**: 71–79. [Medline] [CrossRef]

45. **Yoshida Y, Takahashi K, Okita K, Ichisaka T, Yamanaka S.** Hypoxia enhances the generation of induced pluripotent stem cells. *Cell Stem Cell* 2009; **5**: 237–241. [Medline] [CrossRef]

46. **Chen T, Yuan D, Wei B, Jiang J, Kang J, Ling K, Gu Y, Li J, Xiao L, Pei G.** E-cadherin-mediated cell-cell contact is critical for induced pluripotent stem cell generation. *Stem Cells* 2010; **28**: 1315–1325. [Medline] [CrossRef]

47. **Kirkland SC.** Type I collagen inhibits differentiation and promotes a stem cell-like phenotype in human colorectal carcinoma cells. *Br J Cancer* 2009; **101**: 320–326. [Medline] [CrossRef]

48. **Kirkland SC, Ying H.** Alpha2beta1 integrin regulates lineage commitment in multipotent human colorectal cancer cells. *J Biol Chem* 2008; **283**: 27612–27619. [Medline] [CrossRef]